

# Multiple Satellites Collaboration for Joint Code-aided CFOs and CPOs Estimation

XXX, Member, IEEE,

XXX, Member, IEEE, and XXX, Fellow, IEEE

**Abstract**—Low Earth Orbit (LEO) satellites are being extensively researched in the development of secure Internet of Remote Things (IoRT). In scenarios with miniaturized terminals, the limited transmission power and long transmission distance often lead to low Signal-to-Noise Ratio (SNR) at the satellite receiver, which degrades communication performance. A solution to address this issue is the utilization of cooperative satellites, which can combine signals received from multiple satellites, thereby significantly improve SNR. However, in order to maximize the combination gain, the signal coherent combining is necessary, which requires the carrier frequency and phase of each receiving signal to be aligned. Under low SNR circumstances, carrier parameter estimation can be a significant challenge, especially for short burst transmission with no training sequence. In order to tackle it, we propose an iterative code-aided estimation algorithm for joint Carrier Frequency Offset (CFO) and Carrier Phase Offset (CPO). The Cramér-Rao Lower Bound (CRLB) is suggested as the limit on the parameter estimation performance. Simulation results demonstrate that the proposed algorithm can approach Bit Error Rate (BER) performance bound within 0.4 dB with regards to four-satellite collaboration.

**Index Terms**—Cooperative satellite communication, low signal to noise ratio, short burst transmission, signal coherent combining, carrier frequency offset, carrier phase offset.

## I. INTRODUCTION

Internet of Remote Things (IoRT) is a network of small objects which are often dispersed over wide geographical areas even inaccessible. In IoRT, satellite communication can provide a cost-effective solution to their interconnection and communication in comparison to terrestrial networks [1]–[3]. However, due to the limited link budgets caused by the terminal’s constrained transmission power and long distance between the satellite and terminal, the satellite receiver has to operate at low Signal-to-Noise Ratio (SNR). The reception and processing of low SNR signals has traditionally been a challenging task in signal processing. One attractive approach to addressing this challenge is the use of cooperative diversity techniques. In recent years, Cooperative Satellite Communication (CSC) has garnered significant attention due to its potential to enhance communication reliability and efficiency in satellite networks [4]. This technique is particularly useful for remote or energy-limited terminals, such as those employed in IoRT. With the rapid expansion of Low Earth Orbit (LEO) constellations, it has become feasible to implement collaboration between multiple satellites. Consequently, multi-satellite

signal combining can be an effective strategy to achieve efficient spectral resource utilization and improve communication performance in low SNR environments.

In the context of IoRT systems utilizing CSC, uplink cooperation can facilitate the collaborative reception of signals from a single terminal by multiple satellites. This enables effective signal combination through the integration of received signals. However, due to factors such as varying distances between satellites and terminals, antenna directivity, relative velocities, and crystal oscillator drift on board the satellites, it is possible that signal amplitude, propagation delay, Carrier Frequency Offsets (CFOs), and Carrier Phase Offsets (CPOs) may vary significantly among satellites. If these parameters are not aligned, diversity reception performance may deteriorate, leading to infeasible demodulation. To address this issue, accurate estimation of parameter differences among received signals and optimal combining weights is crucial for successful signal combination. However, with regards to CSC, most existing research has focused on mitigating jamming [5], capacity analysis [6]–[8], and capacity optimization [9]. These studies typically assume that synchronization between satellites and terminals has already been achieved, which is not necessarily the case in practical implementations. To the author’s knowledge, there is no study that has addressed these tasks in detail.

The current studies on estimation of CFOs and CPOs have primarily focused on individual reception scenarios. The estimation methods can be broadly categorized into two approaches: Data-Aided (DA) and Non-Data-Aided (NDA). DA parameter estimation requires the use of a known pilot symbol sequence as a training sequence, which can limit its applicability and reduce the effective data rate and spectral efficiency of the system [10]. NDA estimation does not require additional known data as a training sequence but directly estimates the parameters based on the signal characteristics. However, demodulation noise introduced by NDA methods can degrade synchronization accuracy, especially in low SNR scenarios [11]. Recent studies have focused on Code-Aided (CA) carrier synchronization algorithms that utilize the decoding results from the decoder to estimate the carrier parameters [?], [12], [13]. This innovative approach incorporates coding gain into the carrier synchronization process, leading to enhanced performance, particularly in low SNR scenarios without the need for pilot symbols. The CA technique has demonstrated particularly effective in short-burst communication systems [14], making it a promising approach for applications in IoRT.

Nevertheless, the CA synchronization method also has its

limitations. Firstly, it is subject to significant constraints on the estimation range of both CFO and CPO. As will be illustrated in section III of this paper, in order to achieve decoding performance with a Bit Error Rate (BER) below 0.5, the Normalized Frequency Offset (NFO) must be smaller than  $1e-4$ , while the CPO must fall within the range of  $(-0.2\pi, 0.2\pi]$ . Consequently, the applicability of the CA method is inherently restricted in practical scenarios. To overcome this challenge, a two-dimensional exhaustive search within a narrow NFO range while the CPO is in  $(-\pi, \pi]$  has been proposed in literature [15]. This is coupled with an interpolation algorithm to increase estimation accuracy during the search process. However, due to noise introduced during the single-step search and interpolation processes, as well as the high dependence of algorithm performance on pre-defined thresholds and initial search point selection, there may be a performance degradation at low SNR. Additionally, an algorithm developed in [16] strives to extend the CFO estimation range. It leverages a coarse search and a fine search with code assistance to achieve refined estimation of CFO. However, this Gaussian process remains sensitive to CFO as it is derived from decoding results. Secondly, the CA method exhibits reduced decoding reliability at low SNR levels, resulting in a higher BER during recovery of the modulation information from the transmitted data. This weakens estimation accuracy and highlights the method's sensitivity to CFO and CPO and the reliability of its decoding output. Although the CA synchronization method provides coding gain benefits, its estimation accuracy is limited by the residual frequency bias and random phase bias.

The existing research on CSC lacks sufficient investigation into CFO and CPO estimation. Previous work on CFO and CPO estimation, which focuses on individual reception from a single satellite, has shown improved estimation performance using the CA method without the need for a training sequence. However, this method is not suitable for situations with lower SNR levels and phase offsets within the range of  $(-\pi, +\pi]$  in the CSC scenario. To overcome these limitations, we propose an iterative CA estimation algorithm. It consists of two parts: Iterative Estimation based on Cross Entropy (IECE) and Code-Aided Maximum Likelihood Estimation (CAMLE). The IECE is responsible for coarse search of CFOs and POs, while the CAMLE is responsible for fine estimation of CFOs and CPOs. The proposed algorithm achieves accurate estimation and compensation of CFOs and CPOs, as well as coherent combination of multiple satellites, even under challenging conditions with lower SNR levels and phase offsets within the range of  $(-\pi, +\pi]$  in the CSC scenario. In summary, the contributions of this paper can be outlined as follows:

- We present a general estimation framework for CSC that enables the iterative estimation of CFOs and CPOs without the need for training sequences. It allows for precise estimation of CFOs and CPOs within large residual CFOs and random CPOs in range of  $(-\pi, +\pi]$ . Meanwhile, during each iteration, the combined decoding results are employed to estimate CFOs and CPOs, thereby enhancing the estimation accuracy under the lower SNR condition of each satellite.

- We propose an effective estimation algorithm based on cross entropy. This algorithm enables parallel joint estimation of coarse CFOs and CPOs, taking into account the large residual CFOs and random CPOs inherent in each satellite's range within  $(-\pi, +\pi]$ . During the coarse estimation process, we perform quantization within the potential CFO range and utilize the corrected CFOs to eliminate the received signals from each satellite. Subsequently, we demodulate and square the obtained results to estimate the CPOs. By iteratively combining the signals after CFO and CPO correction in a quasi-coherent manner, using the combining SNR loss as the objective function, we are able to achieve joint estimation of CFOs and CPOs for multiple satellites with only a few iterations.
- We propose a fine MLE algorithm based on Expectation Maximization (EM) iteration to accurately estimate CFOs and CPOs under low SNR conditions. In each iteration, we compensate the received signal at each satellite using the estimated CFO and CPO to achieve coherent combining. The resulting coherent combined decoding results are then utilized to assist in the estimation of CFOs and CPOs. Through several iterations, we obtain accurate estimations of CFOs and CPOs for each satellite, as well as the coherent combined decoding results.

The remainder of this paper is organized as follows. Section II outlines the system model for uplink cooperative satellite communication. Section III formulates the objective function of joint CFOs and CPOs estimation in CSC. In section IV, the iterative estimation algorithm is proposed, which consists of the coarse estimation based on iterative cross entropy and fine estimation based on EM. Section V presents the computation complexity analysis of the proposed algorithms. Simulation results and performance analysis are then shown in Section VI. Ultimately, Section VII draws the conclusions.

## II. SYSTEM MODEL

Direct Sequence Spread Spectrum (DSSS) is widely employed in secure satellite communication systems as it provides inherent resistance against interception, eavesdropping, and interference. Among the various modulation schemes, the Binary Phase Shift Keying-Direct Sequence Spread Spectrum (BPSK-DSSS) modulation scheme has garnered considerable attention owing to its superior performance in noisy environments. To further enhance the reliability of short-burst satellite communication systems operating in noisy channels, Polar codes can be employed. Polar codes belong to a class of error-correcting codes that can approach the Shannon capacity limit even with relatively short code lengths, while maintaining low complexity for both encoding and decoding processes [17], [18]. These codes are particularly suitable for high-reliability communications, especially in scenarios involving short-burst-frame transmission [19]. The transceiver system considered in this paper is depicted in Fig.1.

At the transmitter, the short frame messages to be transmitted are in the form of bit sequence denoted as  $\mathbf{u} = (u_0, u_1, \dots, u_{N-1})^T$ , where  $N$  is the number of the information bits. The information sequence is encoded using a

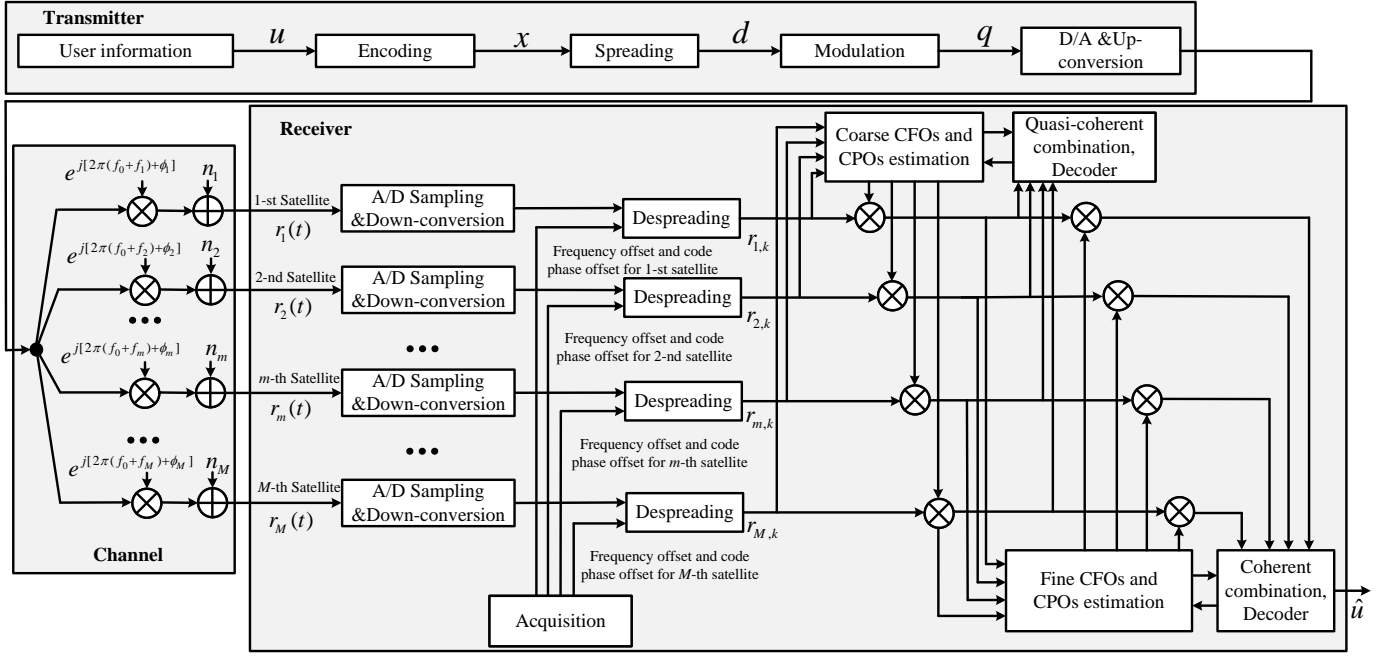


Fig. 1: System architecture of uplink cooperative satellite communication.

binary coder with rate  $R$ , which generates the coded sequence  $\mathbf{x} = (x_0, x_1, \dots, x_{K-1})^T$ . Wherein  $K = N/R$  and  $R < 1$ . Then, the encoded frame is spreaded as  $\mathbf{d}$  with the periodical spreading sequence  $c(\cdot)$ , which the time period is denoted as  $T_c$ . Based on this, the spreaded sequence  $\mathbf{d}$  is modulated into a complex symbol frame  $\mathbf{q} = (q_0, q_1, \dots, q_{KL-1})^T$ , where  $L$  is the length of the periodical spreading sequence and the value of symbols  $\mathbf{q}$  depends on the modulation constellation map.  $q_k = e^{j\pi k} \in \{1, -1\}$  represents the BPSK-modulated symbol. The modulated symbol undergoes frequency up-conversion and D/A conversion. The signal is then transmitted through the wireless channel and is subsequently corrupted by Additive White Gaussian Noise (AWGN).

There are a total of  $M$  satellites in the cooperation network, all of which are capable of receiving the signal transmitted from the same terminal. The wireless channel is assumed to be a line of sight channel. As a result, the received signal by a particular satellite (denoted as  $m$ ,  $m = 1, 2, \dots, M$ ) can be written as:

$$r_m(t) = \sum_{k=0}^{K-1} \sum_{l=0}^{L-1} A_m x_k c(t - lT_c - kT_s) \times e^{j(2\pi(f_0+f_m)t+\phi_m)} + n_m(t), \quad (1)$$

where  $T_s$  is the symbol time duration, and the relation between  $T_c$  and  $T_s$  is  $T_s = L \cdot T_c$ .  $f_0$ ,  $f_m$  and  $\phi_m$  represents the signal carrier frequency, CFO and CPO, respectively. The CFO is determined primarily by the Doppler shift, while the range of CPO varies in the interval  $(-\pi, +\pi]$  due to the differences in start-up time and the drift of crystal oscillators among the collaborating satellites. The term  $n_m(t)$  represents the complex additive Gaussian white noise at satellite  $m$ , with a zero mean and a variance of  $\frac{N_m}{2}$  for both the real and imaginary components. It is assumed that the noise at each

satellite is independent and uncorrelated, with equal variance. The variable  $A_m$  denotes the received signal power from the  $m$ -th satellite. Throughout this paper, it is assumed that the received signal powers are equal for all satellites. Considering that the noise powers are also identical at each satellite, the SNR of the received signal is assumed to be uniform across all satellites.

At the receiver, the first step in signal processing is acquisition. Typically, a low symbol rate  $R_s$  is employed during acquisition to ensure accurate signal detection while satisfying the SNR requirements. Once successful signal acquisition has been accomplished for each satellite and a preliminary estimation of the carrier frequency has been obtained. The received signal at chip level after frequency compensation becomes:

$$r_m(t) = \sum_{k=0}^{K-1} \sum_{l=0}^{L-1} A_m x_k c(t - lT_c - kT_s) \times e^{j(2\pi\Delta f_m t + \phi_m)} + n_m(t). \quad (2)$$

To strike a balance between acquisition probability and resource consumption, the residual CFO after compensation based on the acquisition operation is  $\Delta f_m \in (-\frac{R_s}{2I}, +\frac{R_s}{2I}]$ , where  $I$  represents the number of FFT points utilized in the algorithm mentioned in [20]. Consequently, the remaining NFO, obtained by multiplying the CFO with the symbol period  $T_s$  is reduced to a range of  $\text{NFO}_m \in (-\frac{1}{2I}, +\frac{1}{2I}]$ . The primary objective of this paper is to evaluate the performance of CFO and CPO estimation. To focus on these specific parameters, it is assumed that perfect timing recovery during despreading has been achieved and the signal amplitude has been normalized. Therefore,  $r_m(t)$  is considered as BPSK modulation. After sampling, the  $k$ -th baseband complex symbol can be written

as:

$$r_{m,k} = s_k e^{j(2\pi k \Delta f_m T_s + \phi_m)} + n_m(k). \quad (3)$$

where  $s_k$  is the equivalent BPSK transmitted  $k$ -th symbol after despreading. The  $k$ -th received signal symbol vector  $\mathbf{r}_k$  of all the  $M$  satellites can be described as,

$$\mathbf{r}_k = [r_{1,k}, r_{2,k}, \dots, r_{M,k}]^T. \quad (4)$$

Thus, the received symbol vector of of all the  $M$  satellites is:

$$\mathbf{r} = [\mathbf{r}_0^T, \mathbf{r}_1^T, \dots, \mathbf{r}_{K-1}^T]^T. \quad (5)$$

### III. PROBLEM FORMULATION

Accurately estimating the CFOs and CPOs of all the  $M$  satellites is essential for achieving coherent combination in cooperative satellite communication. These parameters can be denoted as:

$$\begin{aligned} \boldsymbol{\theta} &= [\text{NFO}_1, \dots, \text{NFO}_m, \text{NFO}_M, \phi_1, \phi_2, \dots, \phi_M]^T \\ &= [\mathbf{f}, \boldsymbol{\phi}]^T. \end{aligned} \quad (6)$$

Maximum Likelihood Estimation (MLE) is a well-established and effective technique used to solve parameter estimation problems. This method involves computing the probability density function of the parameter being estimated. In the context of cooperative satellite communication, where the received signals from each satellite are encoded and modulated using identical information bit sequences, and the noise in each satellite is both independent and unrelated, the conditional probability density function of the symbol can be expressed as (7).

By removing the constant component, which is irrelevant to the parameter estimation, (7) can be simplified to:

$$p(\mathbf{r}_k | \boldsymbol{\theta}, s_k) = \exp \left\{ \sum_{m=1}^M \frac{2\Re [s_k^* e^{-j(2\pi k \Delta f_m T_s + \phi_m)} r_{m,k}]}{N_m} \right\}. \quad (8)$$

The data symbol  $s_k$  is an independent and identically distributed discrete random variable, and its probability function can be represented as  $p_s(s_k)$ . By applying the law of total probability and (8), the probability density function of the  $k$ -th symbol vector  $\mathbf{r}_k$  can be derived as:

$$\begin{aligned} p(\mathbf{r}_k | \boldsymbol{\theta}) &= \mathbb{E}_{s_k} [p(\mathbf{r}_k | \boldsymbol{\theta}, s_k)] \\ &= \sum_{\mathbf{m}=0}^{\mathfrak{M}-1} p_k(\mathbf{m}) p(\mathbf{r}_k | \boldsymbol{\theta}, s_k). \end{aligned} \quad (9)$$

$\mathfrak{M}$  represents the modulation order. In terms of BPSK-modulated signal,  $\mathfrak{M} = 2$  and it has

$$p_k(\mathbf{m}) = \frac{1}{2}, \mathbf{m} = \{0, 1\}. \quad (10)$$

Combining (8) to (10), the probability density function of the  $k$ -th data vector  $\mathbf{r}_k$  is expressed as:

$$p(\mathbf{r}_k | \boldsymbol{\theta}) = \cosh \left\{ \sum_{m=1}^M \frac{2\Re [e^{-j(2\pi k \Delta f_m T_s + \phi_m)} r_{m,k}]}{N_m} \right\}. \quad (11)$$

Due to the independence of  $s_k$ , the probability density function of data vector of all the  $M$  satellites is written as:

$$\begin{aligned} p(\mathbf{r} | \boldsymbol{\theta}) &= \prod_{k=0}^{K-1} p(\mathbf{r}_k | \boldsymbol{\theta}) \\ &= \prod_{k=0}^{K-1} \left\{ \cosh \left\{ \sum_{m=1}^M \frac{2\Re [e^{-j(2\pi k \Delta f_m T_s + \phi_m)} r_{m,k}]}{N_m} \right\} \right\}. \end{aligned} \quad (12)$$

Accordingly, the MLE of  $\boldsymbol{\theta} = [\mathbf{f}, \boldsymbol{\phi}]^T$  can be expressed as:

$$\hat{\boldsymbol{\theta}} = \arg \max_{\boldsymbol{\theta} \in \mathcal{F}} [\ln \Lambda(\mathbf{r} | \boldsymbol{\theta})], \quad (13)$$

where  $\mathcal{F}$  is the range of the parameter  $\boldsymbol{\theta}$ .

It is observed that obtaining the MLE value from the log likelihood function is a challenging and nonlinear optimization problem, primarily due to non-linearity, a large search space, and the presence of multiple local minima. These factors make direct solution difficult. In response, researchers have explored iterative approaches to address this issue, such as Simple [21], [22], Simple [21], and Particle Swarm Optimization Frequency and Phase Estimation (PSOFPE) [?]. The SIMPLE algorithm achieves array coherence by employing a simple pair-wise correlation of antenna signals, while the SUMPLE algorithm performs a summation operation on multiple antenna signals prior to correlation. Both algorithms assume perfect compensation of carrier frequency offset and aim to estimate phase deviations through iterative cross-correlation of multi-channel received signals, maximizing combined SNR. Continuous signal updating is required during iteration, making these algorithms more suitable for continuous communication scenarios rather than short-burst communication. To address this limitation, the PSOFPE algorithm has been proposed as an alternative. This algorithm randomly assigns values to carrier frequency and phase offsets, and maximizes equation (13) within a limited data length. However, it falls in the category of NDA method, which results in poor estimation accuracy [23]. On the other hand, the CA method offers comparable estimation accuracy to DA methods, making it more desirable for limited data transmission scenarios. Nonetheless, it is susceptible to residual CFO and CPO, potentially leading to encoding and decoding errors as well as communication failure. Overall, for the considered communication system, there currently is not a suitable solving method available.

### IV. PROPOSED CFO AND CPO ESTIMATION ALGORITHM

To ensure signal coherent combination in cooperative satellite communication system under low SNR conditions, we propose an iterative CA estimation algorithm for jointly estimation CFOs and CPOs. The algorithm consists of two parts: Iterative eEstimation based on Cross Entropy (ICE) and Cooperative Expectation Maximization (CEM). The ICE is responsible for coarse search of CFOs and CPOs, while the CEM is responsible for fine estimation of CFOs and CPOs. The overall structure of these two parts is depicted in Fig.2. The underlying principles of these two parts will be elaborated upon in the following subsections.

$$\begin{aligned}
p(\mathbf{r}_k | \boldsymbol{\theta}, s_k) &= \left( \pi^M \prod_{m=1}^M N_m \right)^{-1} \exp \left\{ - \sum_{m=1}^M \frac{|r_{m,k} - s_k e^{j(2\pi k \Delta f_m T_s + \phi_m)}|^2}{N_m} \right\} \\
&= \left( \pi^M \prod_{m=1}^M N_m \right)^{-1} \exp \left\{ - \sum_{m=1}^M \frac{(|r_{m,k}|^2 - 2\Re [s_k^* e^{-j(2\pi k \Delta f_m T_s + \phi_m)} r_{m,k}] + |s_k|^2)}{N_m} \right\}
\end{aligned} \quad (7)$$

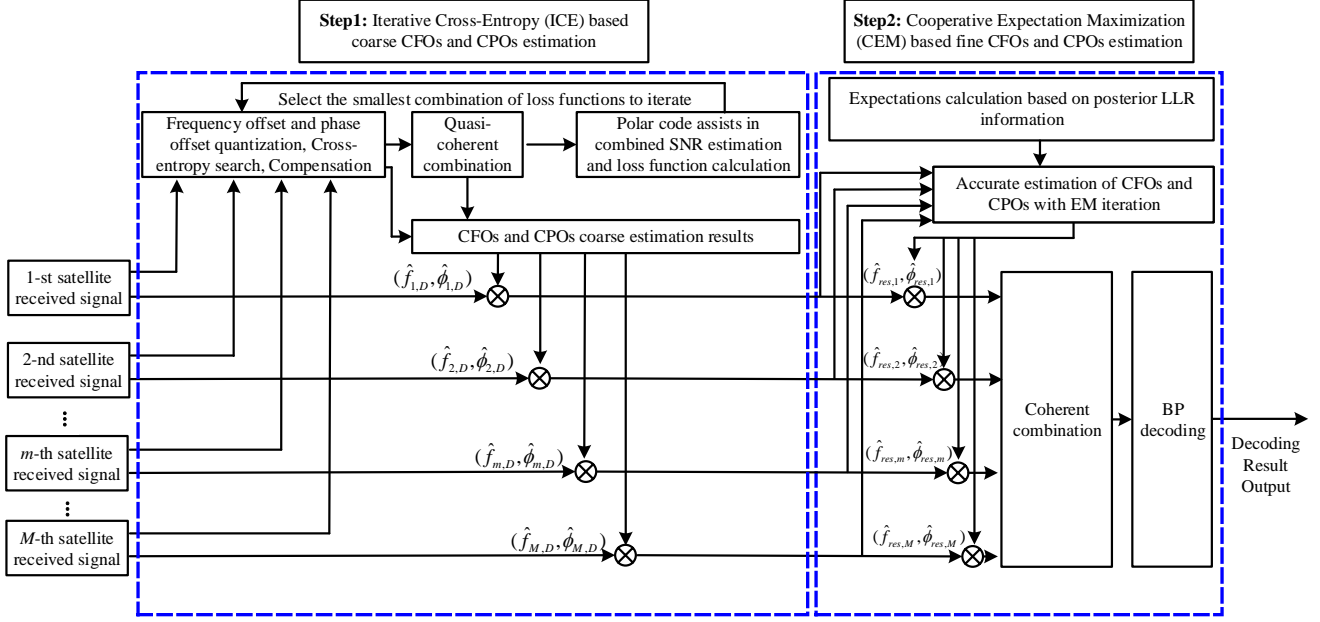


Fig. 2: The schematic diagram of the estimator.

### A. Iterative Cross-Entropy (ICE) based Coarse CFOs and CPOs Estimation

The initialization step of our proposed algorithm involves the utilization of a cross-entropy-based iteration method, which is commonly employed in parameter estimation tasks. This method measures the disparity between the true probability distribution and the predicted probability distribution of a given model, making it an efficient parallel search algorithm. It offers several advantages, including simplicity, ease of implementation, fewer parameters, and expandability, making it suitable for our purposes. In the context of CFO and CPO estimation, our algorithm aims to mitigate the uncertainties associated with their ranges. The CFO range falls within the interval of  $(-\frac{1}{2T}, +\frac{1}{2T}]$ , while the CPO range falls within  $(-\pi, \pi]$ . By applying the cross-entropy method, we can effectively conduct a parallel search to estimate these parameters. Our proposed ICE algorithm is depicted in Fig.3. To handle CFO estimation, we employ quantization with  $D$  bits, which allows us to compensate the received signal at each satellite using the quantized frequency offset. Subsequently, demodulation is performed to calculate the phase offset. However, the square demodulation of a BPSK-modulated signal introduces a phase ambiguity, which we resolve by introducing an additional bit. As a result, the cross-entropy iteration process involves the participation of the received

signal at each satellite using  $D + 1$  bits. During the iteration process, the objective function that drives the iteration and defines the convergence condition is the combined SNR loss. We select the optimal CFOs and CPOs when the objective function reaches its minimum. Accurate SNR estimation is crucial for optimization; hence, we incorporate a Polar code-aided estimation algorithm to enhance the precision of SNR estimation. By employing this approach, we can successfully complete the joint search for CFOs and CPOs of multiple satellites within a few iterations.

1) *Objective Function:* Let  $\mathbf{b}_{1 \times M(D+1)} = [b_1, b_2, \dots, b_m, b_M]$  represent the quantized binary set of CFOs and CPOs of the received signal at all  $M$  satellites. Here  $\mathbf{b}_m = [b_{m,1}, b_{m,2}, \dots, b_{m,d}, b_{m,D}, b_{m,\phi}]_{1 \times (D+1)}$ , with  $b_{m,d} \in [0, 1]$ , represents the  $D + 1$  bits quantized binary set of the  $m$ -th satellite,  $d \in [1, D]$ . Besides,  $b_{m,\phi} \in [0, 1]$  represents the quantized value of the CPO of the received signal at the  $m$ -th satellite. For simplicity, let  $l = 1, 2, \dots, M(D + 1)$  represent the index of the quantized bit. After combining the signals, the  $k$ -th symbol is recorded as  $r_{com,k}$ , which can be expressed in detail as:

$$r_{com,k} = \sum_{m=1}^M r_{m,k} e^{-j[2\pi f_{m,d} k T_s + (2b_{m,\phi} - 1)\pi + \phi_{m,d}]}, \quad (14)$$

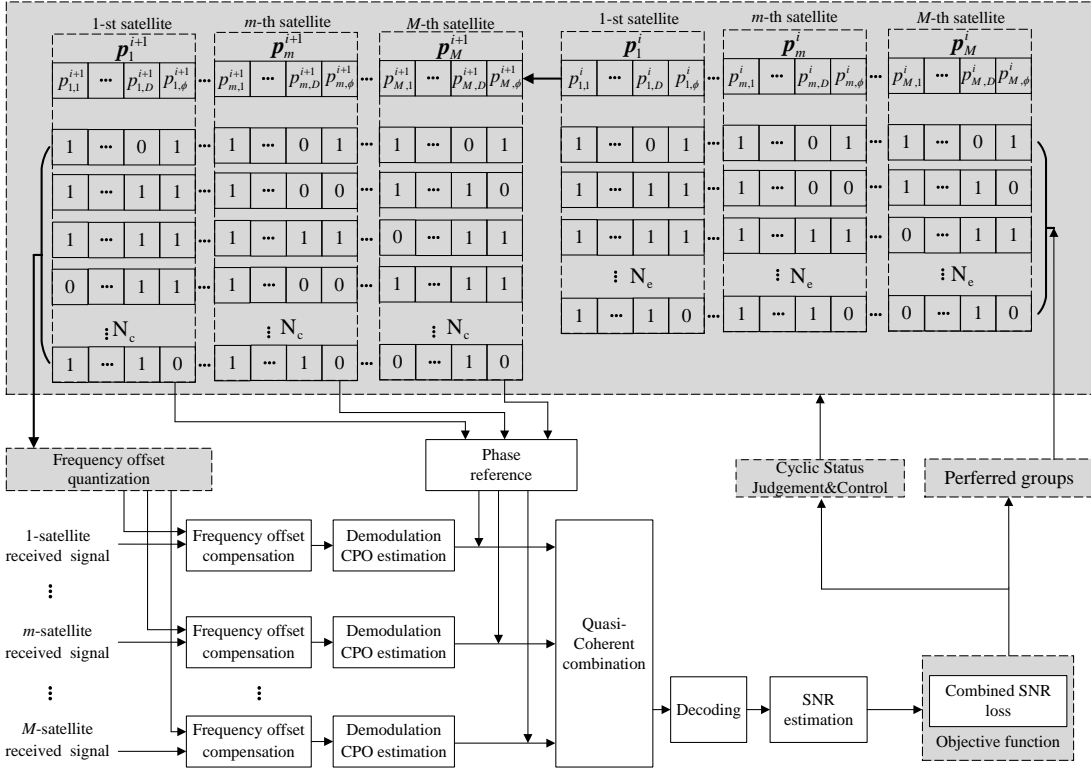


Fig. 3: The schematic diagram of the ICE algorithm.

where  $f_{m,d}$  is the CFO estimation of the received signal at the  $m$ -th satellite. In this case,  $f_{m,d}$  is written as:

$$f_{m,d} = \left( \sum_{d=1}^D 2^{b_{m,d}} - 2^D \right) \frac{R_s}{I2^D}. \quad (15)$$

Additionally,  $\phi_{m,d}$  in (14) is the compensated result of the received signal at the  $m$ -th satellite, which is expressed by:

$$\phi_{m,d} = \frac{1}{2} \arg \left( \sum_{k=0}^{K-1} r_{m,k}^2 e^{-j2\pi 2f_{m,d} k T_s} \right). \quad (16)$$

In order to eliminate the phase ambiguity and achieve coherent combination, each satellite introduces 1 bit to indicate selection between  $\phi_{m,d}$  and  $\phi_{m,d} + \pi$ .

Assuming that the SNR of each satellite as  $\text{SNR}_{\text{Single}}$ , the theoretical SNR after coherent combination is given by  $\text{SNR}_{\text{Single}} + 10 \log_{10}(M)$ . In this context, the measure of combined SNR loss can be expressed as a function involving the estimated combined SNR  $\hat{\gamma}$ :

$$\text{SNRLoss} = \text{SNR}_{\text{Single}} + 10 \log_{10}(M) - \hat{\gamma}, \quad (17)$$

The calculation of the estimated combined SNR of a BPSK-modulated signal using the CA method can be expressed as:

$$\hat{\gamma} = \frac{\left( K - \frac{3}{2} \right) \left( \sum_{k=0}^{K-1} \Re \{ r_{\text{com},k} \zeta_k^* \} \right)^2}{K \left\{ K \left( \sum_{k=0}^{K-1} |r_{\text{com},k}|^2 \right) - \left( \sum_{k=0}^{K-1} \Re \{ r_{\text{com},k} \zeta_k^* \} \right)^2 \right\}}, \quad (18)$$

Where  $\zeta_k$  is the posterior expectation of the  $k$ -th combined signal, and the symbol  $*$  denotes the conjugation operation.

The objective function aims to minimize the SNR loss by finding the optimal binary set  $\mathbf{b}$ , namely:

$$\hat{\mathbf{b}} = \arg \min_{\mathbf{b} \in \mathcal{B}} (\text{SNRLoss} < T_H), \quad (19)$$

Here, the notation  $T_H$  represents the threshold value. Additionally,  $\mathcal{B}$  denotes the complete set of quantized CFOs and CPOs of all  $M$  satellites.

2) *Algorithm Design*: The parameter  $\zeta_k$  in (18) can be calculated by the posterior Log-Likelihood Ratio (LLR) from the output of the decoder. The posterior probability of the encoded data  $x_k$  is expressed as:

$$L_{\text{pos}}(x_k) = \ln \frac{\Pr \{ x_k = 0 | r_{\text{com},k} \}}{\Pr \{ x_k = 1 | r_{\text{com},k} \}}, \quad (20)$$

without loss of generality, for BPSK-modulated signal, there is:

$$\Pr \{ s_k = e^{j \cdot 0 \cdot \pi} | r_{\text{com},k} \} = \Pr \{ x_k = 0 | r_{\text{com},k} \}, \quad (21)$$

$$\Pr \{ s_k = 0 | r_{\text{com},k} \} + \Pr \{ x_k = 1 | r_{\text{com},k} \} = 1. \quad (22)$$

By combining equations (20)-(22), we can derive the conditional probability of  $s_k = e^{j \cdot 0 \cdot \pi}$  given  $r_{\text{com},k}$  as:

$$\Pr \{ s_k = e^{j \cdot 0 \cdot \pi} | r_{\text{com},k} \} = \frac{e^{L_{\text{pos}}(x_k)}}{e^{L_{\text{pos}}(x_k)} + 1}. \quad (23)$$

Similarly, the conditional probability of  $s_k = e^{j \cdot 1 \cdot \pi}$  given  $r_{\text{com},k}$  can be expressed as:

$$\Pr \{ s_k = e^{j \cdot 1 \cdot \pi} | r_{\text{com},k} \} = \frac{1}{e^{L_{\text{pos}}(x_k)} + 1}. \quad (24)$$

Base on this, by combining (23) and (24), the expectation of  $\zeta_k$  can be described as:

$$\begin{aligned}\zeta_k &= e^{j \cdot 0 \cdot \pi} \cdot \Pr \{s_k = e^{j \cdot 0 \cdot \pi} | r_{\text{com},k}\} \\ &\quad + e^{j \cdot 1 \cdot \pi} \cdot \Pr \{s_k = e^{j \cdot 1 \cdot \pi} | r_{\text{com},k}\} \\ &= 1 \cdot \frac{e^{L_{\text{pos}}(x_k)}}{e^{L_{\text{pos}}(x_k)} + 1} + (-1) \cdot \frac{1}{e^{L_{\text{pos}}(x_k)} + 1} \\ &= \frac{e^{L_{\text{pos}}(x_k)} - 1}{e^{L_{\text{pos}}(x_k)} + 1} \\ &= \tanh \left( \frac{e^{L_{\text{pos}}(x_k)}}{2} \right),\end{aligned}\quad (25)$$

where  $\tanh$  represents the hyperbolic tangent function, namely,  $\tanh(x) = \frac{e^x - e^{-x}}{e^x + e^{-x}}$ . The computation of the hyperbolic tangent function involves a relatively high complexity. To mitigate this, a common approach is to approximate it using a linear piecewise function. This approximation can be mathematically represented as:

$$\zeta_k = \begin{cases} 1, & L_{\text{pos}}(x_k) > T_h \\ \alpha L_{\text{pos}}(x_k), & -T_h < L_{\text{pos}}(x_k) \leq T_h \\ -1, & L_{\text{pos}}(x_k) \leq -T_h, \end{cases}\quad (26)$$

where  $L_{\text{pos}}(x_k)$  indicates the posterior LLR of the  $k$ -th symbol  $r_{\text{com},k}$ ,  $\alpha$  represents the linear factor, and  $T_h$  denotes the segmentation point. To achieve a more accurate approximation of the hyperbolic tangent function, the value of  $\alpha$  is set to  $1/3$  and  $T_h$  is set to 3, as suggested in the literature [24].

In Fig. 3, the probability vector for the  $i$ -th iteration process is defined as  $\mathbf{p}_{1 \times M(D+1)}^i = [\mathbf{p}_1^i, \dots, \mathbf{p}_m^i, \dots, \mathbf{p}_M^i]$ . Here  $\mathbf{p}_m^i$  represents the probability of CFO and CPO  $D+1$  bits quantization of the  $m$ -th satellite. To simplify the notation, we denote  $p_l^i$  an element in  $\mathbf{p}^i$ , where  $l \in 1, \dots, M(D+1)$ . Subsequently, the probability vector  $\mathbf{p}_{1 \times M(D+1)}^i$  is utilized to randomly generate a set of candidate observation matrices  $\{\mathbf{B}\}_{n_c=1}^{N_c}$ . Here  $N_c$  denotes the number of vectors. These  $N_c$  groups of candidate vectors are then combined with multiple satellites using equations (14)-(16), and the objective function is calculated to obtain the combined SNR loss vector  $\text{SNRLossVec}_{1 \times N_c}$ . Based on this, the combined SNR loss vector is arranged in ascending order as  $\eta_{\text{seq},1}^i \leq \eta_{\text{seq},2}^i \leq \dots \leq \eta_{\text{seq},N_c}^i$ . The  $N_e$  vectors with the smallest combined SNR loss are then selected and recorded as  $\{\mathbf{B}\}_{n_c=d_{e,1}}^{n_c=d_{e,N_e}}$ , where  $d_{e,n_e}$  represents the index of the selected vectors. Subsequently, the probability generation vector is updated based on these indices.

$$\mathbf{p}^{i+1} = (1 - \bar{w})\mathbf{p}^i + \frac{\bar{w}}{N_e}(\mathbf{b}_{d_{e,1}} + \mathbf{b}_{d_{e,2}} + \dots + \mathbf{b}_{d_{e,N_e}}), \quad (27)$$

By introducing a smoothing parameter  $\bar{w}$ , the iterative process is carried out for a total of  $N_{\text{iter}}$  iterations to obtain the optimal solution  $\mathbf{b}^*$ . Based on this, the estimated matrix  $\hat{\Phi}_D = [\hat{\mathbf{f}}_D, \hat{\Phi}_D]^T$  can be obtained. Here  $\hat{\mathbf{f}}_D = [\hat{f}_{1,d}, \hat{f}_{2,d}, \dots, \hat{f}_{m,d}, \hat{f}_{M,d}]$  and  $\hat{\Phi}_D = [\hat{\phi}_{1,d}, \hat{\phi}_{2,d}, \dots, \hat{\phi}_{m,d}, \hat{\phi}_{M,d}]$  represent the estimated CFO and CPO parameters for each satellite. The algorithmic procedure described above is summarized in Algorithm 1.

---

**Algorithm 1:** ICE algorithm

---

**Input:**  $N_c, N_e, N_{\text{iter}}$ , received signal of all  $M$  satellites  $\mathbf{r} = [\mathbf{r}_1, \mathbf{r}_2, \dots, \mathbf{r}_M]^T$

**Output:**  $\hat{\mathbf{b}}, \hat{\Phi}_D$

Initialization: Set the initial probability for the CFOs and CPOs quantized bits of each satellite as

$\mathbf{p}^i = 0.5 * \mathbf{1}_{1 \times M(D+1)}$ , where  $i = 0$ ;

**while**  $i \leq N_{\text{iter}} - 1$  **do**

- (1) Generate observation matrices  $\{\mathbf{B}\}_{n_c=1}^{N_c}$  to obtain the quantized CFOs and CPOs of received signal symbol at each satellite according to (15) and (16);
- (2) Calculate the combined SNR loss denoted as  $\text{SNRLossVec}_{1 \times N_c}$ , and mark its elements as  $\eta_1^i, \eta_2^i, \dots, \eta_{N_c}^i$ ;
- (3) Sort the elements in ascending order and update it as  $\eta_{\text{seq},1}^i \leq \eta_{\text{seq},2}^i \leq \dots \leq \eta_{\text{seq},N_c}^i$ ;
- (4) Select the top  $N_e$  with the smallest combined SNR loss and calculate the iteration probability of the next iteration by  $\mathbf{p}^{i+1} = (1 - \bar{w})\mathbf{p}^i + \frac{\bar{w}}{N_e}(\mathbf{b}_{d_{e,1}} + \mathbf{b}_{d_{e,2}} + \dots + \mathbf{b}_{d_{e,N_e}})$ ;
- (5)  $i = i + 1$ ;

**end**

return:  $\hat{\mathbf{b}}, \hat{\Phi}_D$

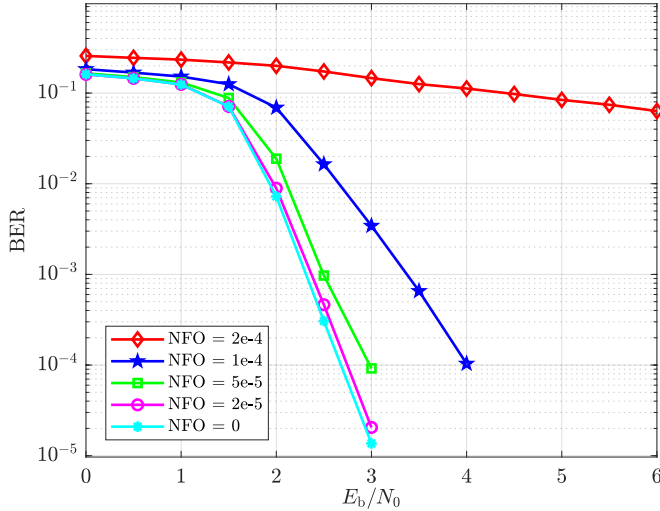
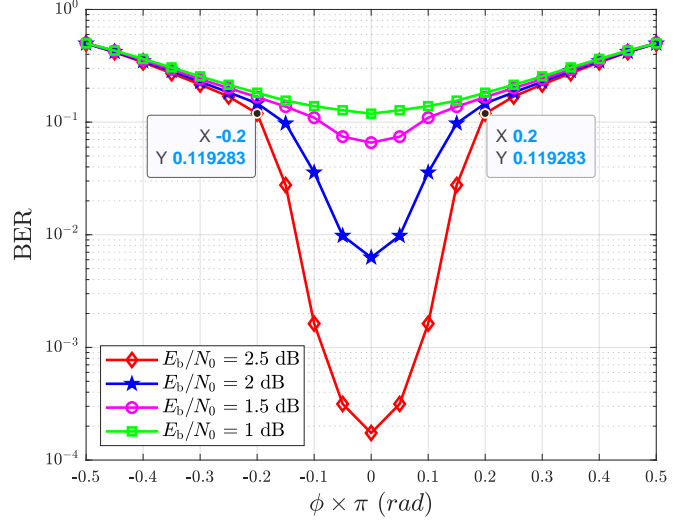
---

3) *Performance Simulation:* According to the aforementioned algorithm design, the selection of parameters such as the frequency offset quantization bit width  $D$ , the number of candidate vectors  $N_c$ , the number of elite vectors  $N_e$ , and the number of iterations  $N_{\text{iter}}$  is an open question that needs to be determined. In order to analyze the impact of these parameters on the algorithm performance, we conduct simulations using the ICE algorithm for joint estimation of CFOs and CPOs.

The choice of quantization bit width for the frequency offset requires finding a balance between system performance and complexity. To illustrate the impact of CFO and CPO on the decoding performance of Polar code  $\mathcal{C}(1024,512)$  using the Belief Propagation (BP) decoding algorithm [25], we perform simulations and the obtained results are shown in Fig. 4. Fig. 4(a) demonstrates that even with a small frequency offset value (NFO =  $1 \times 10^{-4}$ ), there is already a noticeable degradation of more than 1 dB in the decoding performance (@BER =  $10^{-4}$ ) compared to the ideal case. As the NFO further increases, the decoding performance deteriorates gradually. When NFO =  $2 \times 10^{-4}$  and  $E_b/N_0 = 1.5$  dB, the BER approaches 0.5, indicating a significant degradation in the decoding performance and rendering the decoder ineffective. In Fig. 4(b), the impact of CPO on the BER is illustrated. It can be observed that even small changes in the phase offset within the range of  $[-0.2\pi, +0.2\pi]$  can have a considerable impact on the BER. Therefore, given the NFO value of  $1 \times 10^{-4}$ , the quantization bit width  $D$  can be determined by:

$$D \geq \left\lceil \log_2 \frac{1}{\text{NFO} \cdot I} \right\rceil, D \in \mathbb{N}^+ \quad (28)$$

When  $R_s = 1000$  sps and  $I = 64$ , the range of NFO for each satellite is within the interval  $(-7.8125 \times 10^{-3}$ ,

(a) BER versus  $E_b/N_0$  at varying normalized frequency offsets(b) BER versus phase offset at varying  $E_b/N_0$ Fig. 4: The impact of CFO and CPO on the decoding performance of Polar code  $\mathcal{C}(1024,512)$ 

$+7.8125 \times 10^{-3}$ ]. In the simulation presented in Fig. 5, we consider a random combination of  $N_c = 120$  with a candidate group size of  $N_e = 24$ . We investigate the relationship between the combined SNR of multiple satellites and the SNR of a single satellite under different frequency offset quantization bit conditions. As shown in Fig. 5, when the frequency offset quantization bit width is set to 5, the combined SNR loss for CSC with 4 and 6 satellites in collaboration is approximately 4.2 dB and 4 dB, respectively. However, when the quantization bit width is increased to 7, the combined SNR loss for these two cases is reduced to 0.5 dB and 0.4 dB, respectively. It can be observed that increasing the quantization bit width improves the combined SNR, bringing it closer to its theoretical value. However, a higher quantization bit width also results in increased computational complexity. To strike a balance between combining performance and computational complexity, we choose a frequency offset quantization bit width of 6 bits for the subsequent simulations in this paper. This choice provides a reasonable compromise between achieving satisfactory combining performance and managing computational complexity effectively. Then, the relationship between the combined SNR loss and the number of iterations is simulated. Simulation parameters are set as  $D = 6$ ,  $E_s/N_0 = -3$  dB, the number of satellites  $M = 4$ , the range of CFO of received signal at each satellite  $(-7.8125 \times 10^{-3}, +7.8125 \times 10^{-3})$ . As can be seen from the Fig. 6, when  $N_e = 4$ , it takes 4 iterations to converge, and the combined SNR loss is about 1.3 dB. when  $N_e = 32$ , it takes 8 iterations to converge, and the combined SNR loss is only 0.4 dB. This is because when the number of optimal combinations is small, although the convergence rate is faster, it is possible to obtain the local optimal solution. With the increase of  $N_e$ , the global optimal solution can be obtained and the small Combined SNR loss can be obtained. However, the number of iterations also increases, resulting in an increase in computation. To select the appropriate number of optimal combinations, it is necessary to ensure that the

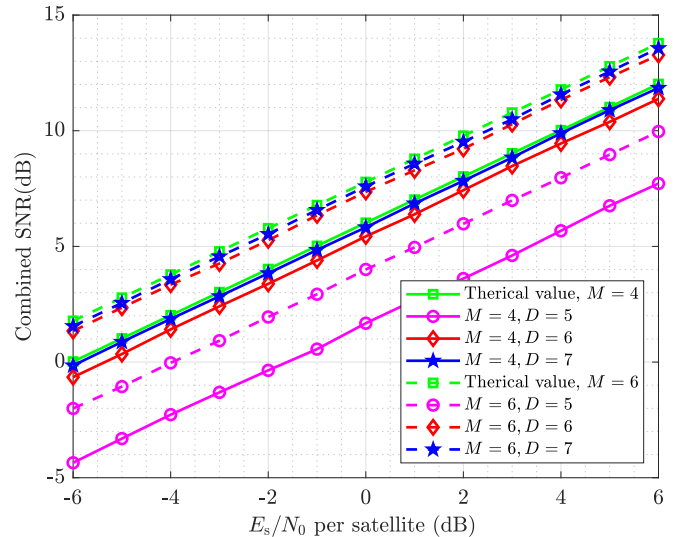


Fig. 5: The relationship between combined SNR and single satellite SNR for varying frequency offset quantization bit widths in the context of multiple satellite systems.

combined SNR loss converges to the global optimal solution under the condition of not increasing too much computation.

Given  $D = 6$ ,  $E_s/N_0 = -3$  dB, Fig.7 shows the relationship between the number of random combinations and the combined SNR loss. It can be seen from Fig.7 that the more combinations are combined in each iteration, the larger the range of both CFOs and CPOs at each iteration, and it is more possible to converge to the optimal value. However, when the number of random combinations reaches the 120 group, the optimal value that converges tends to stabilize, and further increasing the number of random combinations will increase the complexity. Additionally, Fig.7 also depicts the relationship between the number of random combinations and the number of optimal combinations. When the number of

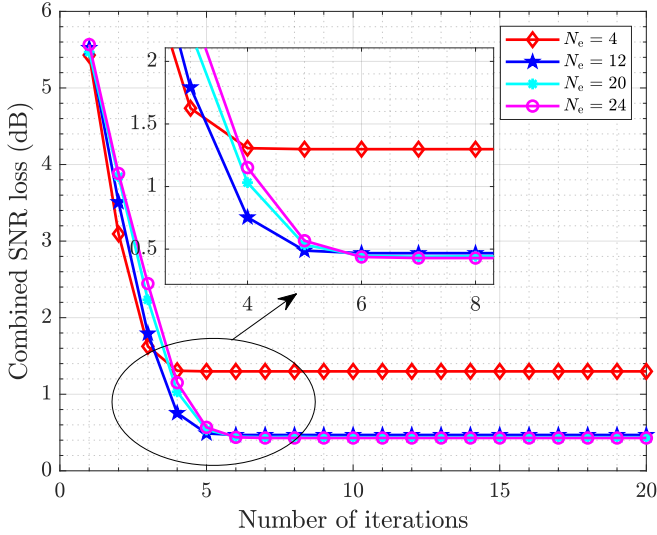


Fig. 6: The relationship between  $N_c$ ,  $N_e$  and the iterations times

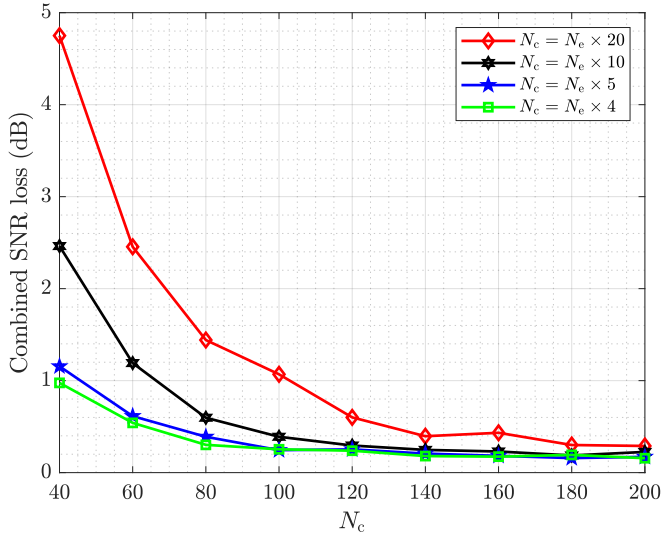


Fig. 7: The relationship between  $N_c$  and  $N_e$

optimal combinations is small, it is easy to converge to the local optimal value. When the number of optimal signal combinations is  $1/5$  of the number of random signal combinations, it is more possible to obtain the optimal solution.

### B. Cooperative Expectation Maximization (CEM) based Fine CFOs and CPOs Estimation

1) *Objective Function:* Although the ICE algorithm reduces CFO of each satellite from  $(-\frac{1}{2T}, +\frac{1}{2T}]$  to  $(-\frac{1}{2D+1T}, +\frac{1}{2D+1T}]$ , it is not possible to obtain accurate estimation results of CFOs and CPOs because of the frequency offsets quantization of each satellite. Based on this, An MLE method are proposed to further accurately estimate the residual CFOs and CPOs after the compensation by the ICE algorithm to complete the coherent combination among satellites.

From (13), it is difficult to solve MLE value by using direct derivation method. As a remedy, the EM algorithm iterates the

estimation parameters by assuming the hidden variables and finally obtains the MLE value [26]. The estimation results of the CFOs and CPOs obtained from the ICE algorithm are used to compensate received signals of each satellite. In this case, the residual CFOs and CPOs set is denoted as  $\theta_{\text{res}}$ , which can be written as:

$$\begin{aligned} \theta_{\text{res}} &= [f_{\text{res},1}, \phi_{\text{res},1}; \dots; f_{\text{res},m}, \phi_{\text{res},m}; \dots; f_{\text{res},M}, \phi_{\text{res},M}] \\ &= [\Phi_1; \Phi_2; \Phi_m; \dots; \Phi_M]. \end{aligned} \quad (29)$$

The joint density function of the compensated received signal  $\mathbf{r}_m$  for the  $m$ -th satellite is expressed as (30), and  $\Phi_m = [f_{\text{res},m}, \phi_{\text{res},m}]$  represents the residual CFOs and CPOs to be estimated for the  $m$ -th satellite. Similar to (9), after removing the influence of the transmitted data  $\mathbf{s}$ , the resulting conditional probability density function is solely dependent on the parameters  $\Phi_m = [f_{\text{res},m}, \phi_{\text{res},m}]$ . Based on this, (30) can be updated as follows:

$$\begin{aligned} p(\mathbf{r}_m | \Phi_m) &= \mathbb{E}_{\mathbf{s}} [p_k(\mathbf{m}) p(\mathbf{r}_m | f_{\text{res},m}, \phi_{\text{res},m}, \mathbf{s})] \\ &= \sum_{\mathbf{m}=0}^{\mathfrak{M}-1} p_k(\mathbf{m}) p(\mathbf{r}_m | f_{\text{res},m}, \phi_{\text{res},m}). \end{aligned} \quad (31)$$

By eliminating the constant terms unrelated to the parameter estimation, the logarithm of the likelihood function can be given by,

$$\begin{aligned} \ln p(\mathbf{r}_m | \Phi_m) &= \sum_{k=0}^{K-1} \ln \left\{ \sum_{\mathbf{m}=0}^{\mathfrak{M}-1} p_k(\mathbf{m}) \right. \\ &\quad \times \left. e^{\Re[s_k^* e^{-j(2\pi k f_{\text{res},m} T_s + \phi_{\text{res},m)}] r_{m,k}] \right\}. \end{aligned} \quad (32)$$

Considering the low SNR environment and equivalent infinitesimals  $\exp(x) \approx 1 + x$ ,  $\ln(1 + x) \approx x$  [16], (32) can be further written as:

$$\begin{aligned} \ln p(\mathbf{r}_m | \Phi_m) &= \sum_{k=0}^{K-1} \ln \left\{ \sum_{\mathbf{m}=0}^{\mathfrak{M}-1} p_k(\mathbf{m}) \right. \\ &\quad \times \left. e^{\Re[s_k^* e^{-j(2\pi k f_{\text{res},m} T_s + \phi_{\text{res},m)}] r_{m,k}] \right\} \\ &\approx \Re \left\{ \sum_{k=0}^{K-1} \sum_{\mathbf{m}=0}^{\mathfrak{M}-1} p_k(\mathbf{m}) \right. \\ &\quad \times \left. s_k^* r_{m,k} e^{-j(2\pi k f_{\text{res},m} T_s + \phi_{\text{res},m)} \right\} \\ &\approx \Re \left\{ \sum_{k=0}^{K-1} \eta_k^* r_{m,k} e^{-j(2\pi k f_{\text{res},m} T_s + \phi_{\text{res},m)} \right\}, \end{aligned} \quad (33)$$

where  $\eta_k = \sum_{\mathbf{m}=0}^{\mathfrak{M}-1} p_k(\mathbf{m}) s_k$  represents the expectation of the transmitted data. However, the prior probability of the transmitted data is unknown, it is not possible to accurately calculate  $\eta_k$ . Therefore, alternative methods must be adopted for estimation.

In this paper, we employ the EM algorithm to address the aforementioned problem. According to the principles of the EM algorithm, for the  $m$ -th satellite, define the parameter of

$$\begin{aligned}
p(\mathbf{r}_m | \Phi_m, \mathbf{s}) &= \left( \pi^K \prod_{k=0}^{K-1} N_m \right)^{-1} \prod_{k=0}^{K-1} \exp \left\{ -\frac{|r_{m,k} - s_k^* e^{j(2\pi k f_{\text{res},m} T_s + \phi_{\text{res},m})}|^2}{N_m} \right\} \\
&= \left( \pi^K \prod_{k=0}^{K-1} N_m \right)^{-1} \prod_{k=0}^{K-1} \exp \left\{ -\frac{|r_{m,k}|^2 - 2\Re [s_k^* e^{-j(2\pi k f_{\text{res},m} T_s + \phi_{\text{res},m})} r_{m,k}] + |s_k|^2}{N_m} \right\} \quad (30)
\end{aligned}$$

interest  $\Phi_m = [f_{\text{res},m}, \phi_{\text{res},m}]$ , observed signal  $\mathbf{r}_m$ , and the hidden signal, which is the transmitted data  $\mathbf{s}$ . Furthermore, define the entire observed signal  $\mathbf{z}_m = [\mathbf{r}_m, \mathbf{s}]$  as the combination of the observed signal and the transmitted data for the  $m$ -th satellite. Hence the steps of the EM algorithm are as follows:

E – step:

$$\begin{aligned}
\mathcal{Q}(\Phi_m; \Phi_m^{(n-1)}) &= \mathbb{E}_{\mathbf{z}_m | \mathbf{r}_m, \Phi_m^{(n-1)}} [\ln p(\mathbf{z}_m | \Phi_m)] \\
&= \int_{\mathbf{s}} p(\mathbf{s} | \mathbf{r}_m, \Phi_m^{(n-1)}) \ln p(\mathbf{z}_m | \Phi_m) d\mathbf{s} \quad (34)
\end{aligned}$$

M – step:

$$\Phi_m^{(n)} = \arg \max_{\Phi_m} \mathcal{Q}(\Phi_m; \Phi_m^{(n-1)}), \quad (35)$$

where  $n$  denotes the  $n$ -th iteration of the EM algorithm, E – step represents the condition given the observed signal and the parameter of interest  $\Phi_m$ . To calculate the expectation  $\mathbb{E}_{\mathbf{z}_m | \mathbf{r}_m, \Phi_m^{(n-1)}} [\ln p(\mathbf{z}_m | \Phi_m)]$  of the conditional probability distribution  $p(\mathbf{s} | \mathbf{r}_m, \Phi_m^{(n-1)})$  of the hidden data  $\mathbf{s}$ , the logarithm of the likelihood function  $\ln p(\mathbf{z}_m | \Phi_m)$  can be given. M – step is maximizing  $\mathcal{Q}(\Phi_m; \Phi_m^{(n-1)})$  to obtain the parameter estimate  $\Phi_m$ , which serves as the updated parameter to estimate  $\Phi_m^{(n)}$  in the next iteration. This iterative process of performing steps E – step and M – step continues until the algorithm converges, achieving the MLE results of CFOs and CPOs. Since the transmitted data  $\mathbf{s}$  and the parameter of interest  $\Phi_m$  are mutually independent,  $\mathcal{Q}(\Phi_m; \Phi_m^{(n-1)})$  can be written as:

$$\begin{aligned}
\mathcal{Q}(\Phi_m; \Phi_m^{(n-1)}) &= \int_{\mathbf{s}} p(\mathbf{s} | \mathbf{r}_m, \Phi_m^{(n-1)}) \ln p(\mathbf{z}_m | \Phi_m) d\mathbf{s} \\
&= \int_{\mathbf{s}} p(\mathbf{s} | \mathbf{r}_m, \Phi_m^{(n-1)}) \ln p(\mathbf{r}_m, \mathbf{s} | \Phi_m) d\mathbf{s} \\
&= \int_{\mathbf{s}} p(\mathbf{s} | \mathbf{r}_m, \Phi_m^{(n-1)}) \ln p(\mathbf{r}_m | \mathbf{s}, \Phi_m) d\mathbf{s} \\
&\quad + \int_{\mathbf{s}} p(\mathbf{s} | \mathbf{r}_m, \Phi_m^{(n-1)}) \ln p(\mathbf{s}) d\mathbf{s}. \quad (36)
\end{aligned}$$

The right-hand side of (36) is independent of the parameter  $\Phi_m$ , hence  $\mathcal{Q}(\Phi_m; \Phi_m^{(n-1)})$  can be simplified as:

$$\mathcal{Q}(\Phi_m; \Phi_m^{(n-1)}) = \int_{\mathbf{s}} p(\mathbf{s} | \mathbf{r}_m, \Phi_m^{(n-1)}) \ln p(\mathbf{r}_m | \mathbf{s}, \Phi_m) d\mathbf{s} \quad (37)$$

according to (30), Substituting  $p(\mathbf{r}_m | \mathbf{s}, \Phi_m)$  into  $\mathcal{Q}(\Phi_m; \Phi_m^{(n-1)})$ ,  $\mathcal{Q}(\Phi_m; \Phi_m^{(n-1)})$  can be updated as (38). Let  $\zeta_k(\mathbf{r}_m, \Phi_m^{(n-1)}) = \sum_{s_k \in \mathfrak{M}} s_k p(s_k | \mathbf{r}_m, \Phi_m^{(n-1)})$  denotes to the posterior expectation of the transmitted data. Since each

satellite receives the same data, the posterior expectation of the combined received signals from the  $m$ -th satellites, denoted as  $\zeta_k$ , is updated as follows:

$$\begin{aligned}
\zeta_k(\mathbf{r}_{\text{com}}, \Phi^{(n-1)}) &= \sum_{s_k \in \mathfrak{M}} s_k p(s_k | \mathbf{r}_{\text{com}}, \Phi^{(n-1)}) \\
&= \sum_{s_k \in \mathfrak{M}} s_k p\left(s_k \mid \sum_{m=1}^M \sum_{k=0}^{K-1} r_{m,k} \right. \\
&\quad \left. \times e^{-j(2\pi k f_{\text{res},m}^{(n-1)} T_s + \phi_{\text{res},m}^{(n-1)})}, \Phi^{(n-1)}\right) \quad (39)
\end{aligned}$$

$f_{\text{res},m}^{(n-1)}$  and  $\phi_{\text{res},m}^{(n-1)}$  represent the residual CFO and CPO of the  $m$ -th satellite in the parameter set  $\Phi^{(n-1)}$  from the  $(n-1)$ -th iteration. (39) reflects the combination gain of multi-satellite cooperation in parameter estimation, as the posterior expectation of the transmitted symbols is calculated based on the combined results of all satellites. Compared to individual satellite calculations, the expectation calculated from the combined results is more reliable. Therefore,  $\mathcal{Q}(\Phi_m; \Phi_m^{(n-1)})$  can be updated as follows:

$$\begin{aligned}
\mathcal{Q}(\Phi_m; \Phi_m^{(n-1)}) &= \Re \left\{ \sum_{k=0}^{K-1} r_{m,k} \zeta_k^*(\mathbf{r}_{\text{com}}, \Phi^{(n-1)}) \right. \\
&\quad \left. \times e^{-j(2\pi k f_{\text{res},m} T_s + \phi_{\text{res},m})} \right\}. \quad (40)
\end{aligned}$$

In fact,  $\mathcal{Q}(\Phi_m; \Phi_m^{(n-1)})$  has the same form as (33), with the difference that  $\eta_k$  is the prior expectation of the transmitted symbols, and  $\zeta_k(\mathbf{r}_{\text{com}}, \Phi^{(n-1)})$  is the posterior expectation of the transmitted symbols obtained from the combined results of  $m$ -th satellites. Similar to equation (26), it can be calculated using the posterior LLR information obtained from the combined decoding results. Update the M – step for finding the maximum value in the array to:

$$\begin{aligned}
\Phi_m^{(n)} &= \arg \max_{\Phi_m} \Re \left\{ \sum_{k=0}^{K-1} r_{m,k} \zeta_k^*(\mathbf{r}_{\text{com}}, \Phi^{(n-1)}) \right. \\
&\quad \left. \times e^{-j(2\pi k f_{\text{res},m}^{(n-1)} T_s + \phi_{\text{res},m}^{(n-1)})} \right\}. \quad (41)
\end{aligned}$$

Base on this, the iterative process of residual CFO and CPO of the  $m$ -th satellite are separately expressed as

$$\begin{aligned}
f_{\text{res},m}^{(n)} &= \arg \max_{f_{\text{res},m}} \left| \sum_{k=0}^{K-1} r_{m,k} \zeta_k^*(\mathbf{r}_{\text{com}}, \Phi^{(n-1)}) e^{-j2\pi k f_{\text{res},m} T_s} \right| \\
\phi_{\text{res},m}^{(n)} &= \arg \left\{ \sum_{k=0}^{K-1} r_{m,k} \zeta_k^*(\mathbf{r}_{\text{com}}, \Phi^{(n-1)}) e^{-j2\pi k f_{\text{res},m}^{(n)} T_s} \right\}, \quad (42)
\end{aligned}$$

$$\begin{aligned}
\mathcal{Q}(\Phi_m; \Phi_m^{(n-1)}) &= \int_{\mathbf{s}} p(\mathbf{s} | \mathbf{r}_m, \Phi_m^{(n-1)}) \sum_{k=0}^{K-1} \left( \Re \left\{ r_{m,k} s_k^* e^{-j(2\pi k f_{\text{res},m} T_s + \phi_{\text{res},m})} \right\} - |s_k|^2 \right) d\mathbf{s} \\
&= \sum_{s_k \in \mathfrak{M}} p(s_k | \mathbf{r}_m, \Phi_m^{(n-1)}) \sum_{k=0}^{K-1} \Re \left\{ r_{m,k} s_k^* e^{-j(2\pi k f_{\text{res},m} T_s + \phi_{\text{res},m})} \right\} \\
&= \Re \left\{ \sum_{k=0}^{K-1} r_{m,k} \left( \sum_{s_k \in \mathfrak{M}} s_k^* p(s_k | \mathbf{r}_m, \Phi_m^{(n-1)}) \right) e^{-j(2\pi k f_{\text{res},m} T_s + \phi_{\text{res},m})} \right\}
\end{aligned} \tag{38}$$

(42) can be solved to obtain  $f_{\text{res},m}^{(n)}$  by quantizing the frequency within a certain range and searching for the maximum value. Due to the output of ICE algorithm, the range of CFO has been reduced from  $(-\frac{1}{2T}, +\frac{1}{2T})$  to  $(-\frac{1}{2D+1T}, +\frac{1}{2D+1T})$ . Each satellite uses the EM algorithm to complete the residual frequency offset search within the range  $(-\frac{1}{2D+1T}, +\frac{1}{2D+1T})$ . Under this setting, a search step of  $f_{\text{step}}$  is used to calculate formulas for the combined results, hence residual CFO and CPO are updated through iteration:

$$\mathbf{r}_{\text{com}}^{(n-1)} = \sum_{m=1}^M \sum_{k=0}^{K-1} r_{m,k}^{(n-1)} e^{-j(2\pi k f_{\text{res},m}^{(n-1)} T_s + \phi_{\text{res},m}^{(n-1)})} \tag{43}$$

$$f_{\text{res},m}^{(n)} = \arg \max_{f_{\text{res},m}} \left| \sum_{k=0}^{K-1} r_{m,k}^{(n-1)} \zeta_k^*(\mathbf{r}_{\text{com}}^{(n-1)}, \Phi^{(n)}) e^{-j2\pi k f_{\text{step}} T_s} \right| \tag{44}$$

$$\phi_{\text{res},m}^{(n)} = \arg \left\{ \sum_{k=0}^{K-1} r_{m,k} \zeta_k^*(\mathbf{r}_{\text{com}}^{(n-1)}, \Phi^{(n)}) e^{-j2\pi k f_{\text{res},m}^{(n)} T_s} \right\}. \tag{45}$$

2) *Algorithm Design*: Through each EM iteration, the estimated results are used to compensate the received signal of each satellite to complete the coherent combination and decoding. Based on this, the posterior LLR information obtained from the decoder are employed to calculate the expectation of the transmitted data. With the increase of the number of iteration, the estimated value of the CFOs and CPOs is gradually close to the real value, meanwhile the reliability of the posterior LLR information of the decoded output after coherent combining is improved.

In summary, the joint use of ICE algorithm and CEM algorithm (abbreviated as ICE-CEM) can conduct the accurate estimation of CFOs and CPOs within the range of  $(-\frac{1}{2T}, +\frac{1}{2T})$  and  $(-\pi, +\pi)$  to accurate estimation to complete coherent combination among satellites. The flow of the ICE-CEM algorithm is shown in Algorithm 2.

## V. SIMULATION AND PERFORMANCE ANALYSIS

In this section, the estimation performance of the proposed ICE-CEM algorithm in terms of CFOs and CPOs are simulated and analyzed.

The Polar code used in the simulation is  $\mathcal{C}(1024, 512)$ . In order to analyze the CFO and CPO estimation performance of the proposed ICE-CEM algorithms, Fig.8 gives the performance of the ICE-CEM algorithm in terms of RMSE and CRLB for the 2 satellites and 4 satellites scenarios, respectively. On the one hand, Fig.8(a) and Fig.8(b) show

---

### Algorithm 2: ICE-CEM algorithm

---

**Input:** Received signal of all  $M$  satellites

$$\mathbf{r} = [\mathbf{r}_1, \mathbf{r}_2, \dots, \mathbf{r}_M]^T$$

**Output:** The estimated results of frequency offset and phase offset for the despread data of the  $m$ -th satellite

$$\hat{\Phi} = [\Delta \hat{f}_1, \dots, \Delta \hat{f}_m, \Delta \hat{f}_M, \hat{\phi}_1, \dots, \hat{\phi}_m, \hat{\phi}_M]$$

and the decoded result after coherent

combining,  $\Delta \hat{f}_m = \Delta \hat{f}_{m,D} + \hat{f}_{\text{res},m}$ ;

$\hat{\phi}_m = \hat{\phi}_{m,D} + \hat{\phi}_{\text{res},m}$ , decoding out  $\hat{\mathbf{u}}$ .

**Initialization:** In ICE algorithm  $N_c$ , optimal group

number  $N_e$ , maximum number of iterations  $N_{\text{iter}}$ ;

maximum number of iterations  $N_{\text{iter,EM}}$ ;

(1) Using ICE algorithm to obtain the estimated results of frequency offset and phase offset for each satellite's decoded data  $\Delta \hat{f}_{m,D}$  and  $\hat{\phi}_{m,D}$ ;

Compensate for the Despread data of each satellite by exploiting  $\Delta \hat{f}_{m,D}$  and  $\hat{\phi}_{m,D}$ ;

**for**  $1 \leq n \leq N_{\text{iter,EM}}$  **do**

(2) Execution formula (43), merge the compensated results for each satellite, complete Polar code decoding, and obtain posterior Log-Likelihood Ratio (LLR) information. Calculate the mathematical expectation  $\zeta_k(\mathbf{r}_{\text{com}}, \Phi^{(n-1)})$  of the transmitted symbol using equation(26);

(3) Executing the equations sequentially (44) and (45) to obtain accurate estimations of residual frequency offset and phase offset for the decoded data of each satellite;

(4)  $n = n + 1$ ;

**end**

return:  $\hat{\Phi}$ , decoding out  $\hat{\mathbf{u}}$

---

that under the same number of cooperative satellites, the estimated RMSEs of the the CFO and CPO of the ICE-CEM algorithm are close to the CRLB with the increase of the SNR, which is due to the fact that the higher the SNR, the higher the reliability of the posteriori LLR information, and the higher the reliability of  $\zeta_k$  calculated according to (26). On the other hand, as the number of cooperative satellites increases, the SNR required for the RMSE approximation of the CRLB by the ICE-CEM algorithm gradually decreases to about 3 dB, which is precisely the cooperation gain brought by the ICE-CEM algorithm. As the number of cooperative satellites increases, its coherent combining SNR becomes

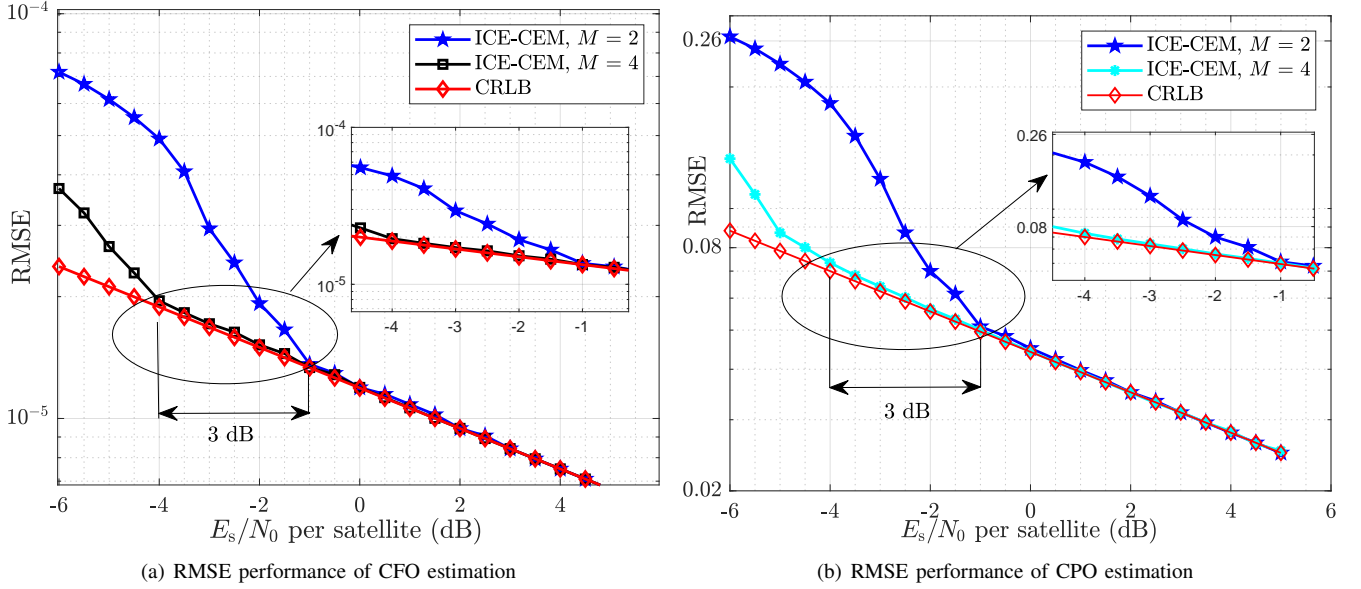


Fig. 8: RMSE performance of CFO and CPO estimation of the ICE-CEM algorithm

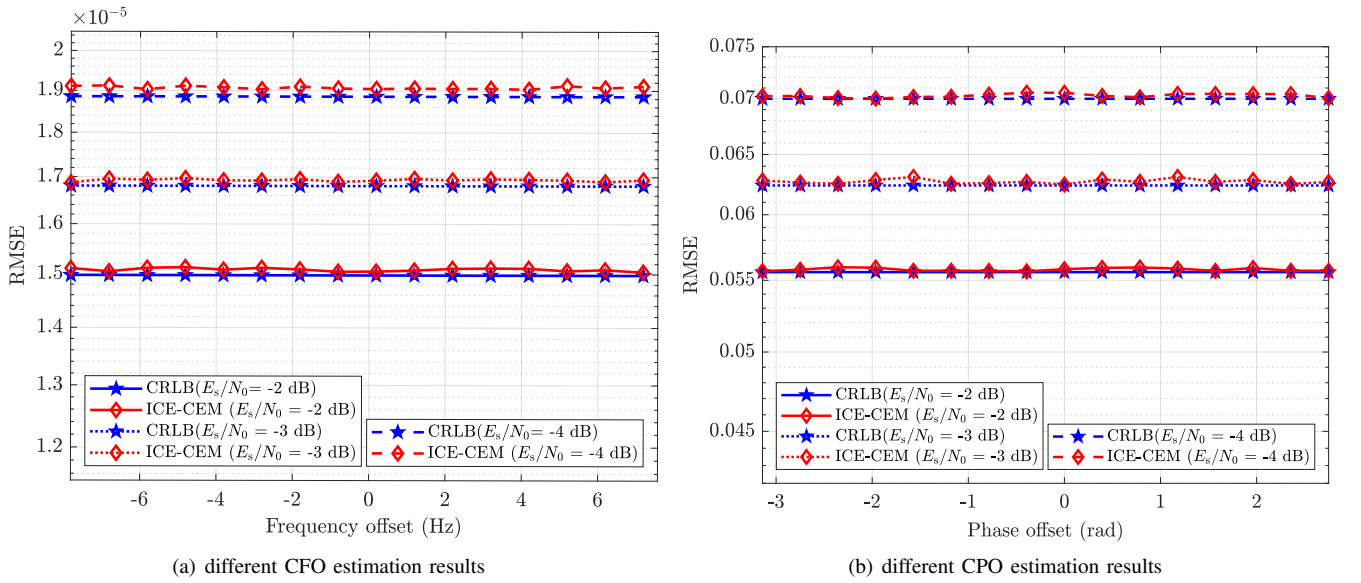


Fig. 9: RMSE performance of 4 satellites, the range of CFO  $(-7.8125 \times 10^{-3}, +7.8125 \times 10^{-3})$ , the range of CPO  $(-\pi, +\pi]$

higher, and the reliability of  $\zeta_k$  after coherent combination becomes higher, resulting in a superior RMSE performance.

Fig.9 shows the estimation performance under different range of CFO and CPO with different  $E_s/N_0$ . Fig.9(a) illustrates the RMSE performance of CFO estimation within the range of  $(-7.8125 \times 10^{-3}, +7.8125 \times 10^{-3})$ . As  $E_s/N_0$  increases, the RMSE of the estimation results gradually approaches the CRLB across the entire range. While Fig.9(b) presents the RMSE performance of CPO within the range of  $(-\pi, +\pi]$ . As the  $E_s/N_0$  increases, the RMSE of the estimation results approaches the CRLB within the entire range.

Finally, the BER simulations can be seen in Fig. 10 with 2 satellites and 4 satellites scenarios. The BER simulation results

are compensated and combined by completing the estimation of the CFOs and CPOs of each satellite. The combined results are decoded using BP decoder. In these two scenarios, the CFO of each satellite is randomly selected in the range of  $(-7.8125 \times 10^{-3}, +7.8125 \times 10^{-3})$ , and the CPO is randomly selected in the range of  $(-\pi, +\pi]$ . It is assumed that the received SNR is same for each satellite. It can be seen from Fig. 10 that the BER performance of the ICE-CEM algorithm incurs the loss of about 0.4 dB and 0.3 dB under 2 and 4 satellites scenarios, respectively ( $@BER=1 \times 10^{-4}$ ). In the 4 satellites scenario, each satellite operates at a lower SNR, and as can be seen from Fig. 8(a) and 8(b), the increase in the RMSE of the CFOs and CPOs estimation for each satellite deteriorates the coherent combination among satellites, which

ultimately leads to a larger loss in the combining decoding performance.

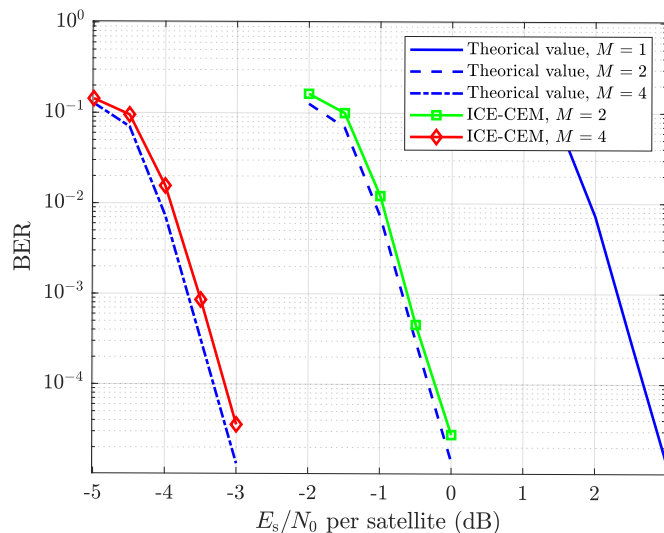


Fig. 10: Simulation results of BER for two-satellite and four-satellite cooperation

## VI. CONCLUSIONS

In this paper, a joint estimation algorithms of CFOs and CPOs for Polar code is proposed, i.e., ICE-CEM, in order to address the problems of large range of CFOs and CPOs estimation and poor synchronization accuracy under low SNR and no training sequences in the multi-satellite cooperation scenario. The proposed algorithm starts with the ICE algorithm to quantize the frequency offset and the random phase offset in the range of  $(-\pi, +\pi]$  for each satellite, and realize the parallel search of the CFOs and CPOs through cross-entropy iteration. On this basis, the CEM algorithm employs the EM iteration algorithm to accurately estimate the CFO and CPO of each satellite.

The simulation results of the RMSE demonstrate that both the estimation range and accuracy exhibit excellent performance. Additionally, the BER simulation results show that the ICE-CEM algorithm in 2 and 4 satellites scenarios occurs only 0.3 dB and 0.4 dB loss ( $@BER=1 \times 10^{-4}$ ).

## REFERENCES

- [1] P. Yue, J. An, J. Zhang *et al.*, “Low Earth orbit satellite security and reliability: Issues, solutions, and the road ahead,” *IEEE Commun. Surveys Tuts.*, vol. 25, no. 3, pp. 1604–1652, Third Quart. 2023.
- [2] P. Yue, J. Du, R. Zhang *et al.*, “Collaborative LEO satellites for secure and green Internet of Remote Things,” *IEEE Internet Things J.*, vol. 10, no. 11, pp. 9283–9294, Jun. 2023.
- [3] M. De Sanctis, E. Cianca, G. Araniti *et al.*, “Satellite communications supporting internet of remote things,” *IEEE Internet Things J.*, vol. 3, no. 1, pp. 113–123, Feb. 2016.
- [4] P.-D. M. Arapoglou, K. P. Liolis, M. Bertinelli *et al.*, “MIMO over satellite: A review,” *IEEE Commun. Surveys Tuts.*, vol. 13, pp. 27–51, First Quart. 2011.
- [5] V. Weerackody, “Satellite diversity to mitigate jamming in LEO satellite mega-constellations,” in *Proc. IEEE International Conference on Communications Workshops*, Montreal, QC, Canada, 14-23 Jun. 2021, pp. 1–6.

- [6] D. Goto, H. Shibayama, F. Yamashita *et al.*, “LEO-MIMO satellite systems for high capacity transmission,” in *Proc. IEEE Global Commun. Conf.*, Abu Dhabi, United Arab Emirates, 9-13 Dec. 2018, pp. 1–6.
- [7] R. Richter, I. Bergel, Y. Noam *et al.*, “Downlink cooperative MIMO in LEO satellites,” *IEEE Access*, vol. 8, pp. 213 866–213 881, Nov. 2020.
- [8] R. Deng, B. Di, and L. Song, “Ultra-dense LEO satellite based formation flying,” *IEEE Trans. Commun.*, vol. 69, no. 5, pp. 3091–3105, May 2021.
- [9] Q. Tang, L. Zhu, T. Li *et al.*, “A high efficient cooperative transmission method for multi-satellite collocation systems,” in *Proc. International Conference on Wireless Communications and Signal Processing*, Nanjing, China, 11-13 Oct. 2017, pp. 1–6.
- [10] M. Morelli and U. Mengali, “Carrier-frequency estimation for transmissions over selective channels,” *IEEE Transactions on Communications*, vol. 48, no. 9, pp. 1580–1589, 2000.
- [11] M. Mohammadkarimi, O. A. Dobre, and M. Z. Win, “Non-data-aided SNR estimation for multiple antenna systems,” in *2016 IEEE Global Communications Conference (GLOBECOM)*, Washington, DC, USA, 04-08 Dec. 2016, pp. 1–5.
- [12] C. Chen, S. Wang, L. Li, S. Ke, C. Wang, and X. Bu, “Intelligent covert satellite communication for military robot swarm,” *IEEE Access*, vol. 8, pp. 5363–5382, 2020.
- [13] F. Bellili, A. Methenni, and S. Affes, “Closed-form CRLBs for CFO and phase estimation from turbo-coded square-QAM-modulated transmissions,” *IEEE Trans. Wirel. Commun.*, vol. 14, no. 5, pp. 2513–2531, May 2015.
- [14] Y. Rahamim, A. Freedman, and A. Reichman, “ML iterative soft-decision-directed (ml-isdd): a carrier synchronization system for short packet turbo coded communication,” *IEEE Transactions on Communications*, vol. 56, no. 7, pp. 1169–1177, 2008.
- [15] X. Man, Z. Xi, K. Gao *et al.*, “A novel code-aided carrier recovery algorithm for coded systems,” *IEEE Commun. Lett.*, vol. 17, no. 2, pp. 405–408, Feb. 2013.
- [16] J. Wang, C. Jiang, L. Kuang *et al.*, “Iterative doppler frequency offset estimation in satellite high-mobility communications,” *IEEE J. Sel. Areas Commun.*, vol. 38, no. 12, pp. 2875–2888, Dec. 2020.
- [17] E. Arikan, “Channel polarization: A method for constructing capacity-achieving codes for symmetric binary-input memoryless channels,” *IEEE Trans. Inf. Theory*, vol. 55, no. 7, pp. 3051–3073, Jul. 2009.
- [18] I. Tal and A. Vardy, “List decoding of polar codes,” *IEEE Trans. Inf. Theory*, vol. 61, no. 5, pp. 2213–2226, May 2015.
- [19] Y. Jing-bao and L. Yu, “Research on reliability design of network nodes in operational command and control system,” in *2017 3rd IEEE International Conference on Computer and Communications (ICCC)*, Chengdu, China, 13-16 Dec. 2017, pp. 724–728.
- [20] P. Tang, S. Wang, X. Li *et al.*, “A low-complexity algorithm for fast acquisition of weak dsss signal in high dynamic environment,” *GPS Solut.*, vol. 4, no. 21, p. 1427–1441, Apr. 2017.
- [21] D. H. Rogstad, “The SUMPLE algorithm for aligning arrays of receiving radio antennas: Coherence achieved with less hardware and lower combining loss,” 2005.
- [22] —, “Aligning an array of receiving radio antennas in the presence of an interfering source: Taking advantage of differences in spectral shape,” 2007.
- [23] X. Du, T. Song, Y. Li *et al.*, “An optimum signal detection approach to the joint ML estimation of timing offset, carrier frequency and phase offset for coherent optical OFDM,” *J. Light. Technol.*, vol. 39, no. 6, pp. 1629–1644, Mar. 2021.
- [24] C. Chen, S. Wang, L. Li *et al.*, “Intelligent covert satellite communication for military robot swarm,” *IEEE Access*, vol. 8, pp. 5363–5382, Dec. 2019.
- [25] H. Liu, E. Gunawan, H. Yaoyue *et al.*, “BP-based sparse graph list decoding of Polar codes,” *IEEE Commun. Lett.*, vol. 27, no. 5, pp. 1257–1261, May 2023.
- [26] X. Li, Q. Wang, J. Sun *et al.*, “Clustering-based blind detection aided by SC-LDGM codes,” *IEEE Trans. Veh. Technol.*, vol. 70, no. 12, pp. 12 771–12 781, Dec. 2021.